J Mol Model (2012) 18:2291–2299
DOI 10.1007/s00894-011-1243-9

ORIGINAL PAPER

Computational investigation of a new ion-pair receptor for calix[4]pyrrole

Yong Xia · Xueye Wang · Yu Zhang · Benhua Luo · Yi Liu

Received: 22 July 2011 / Accepted: 12 September 2011 / Published online: 1 October 2011

Abstract Theoretical studies of a new ion-pair receptor, meso-octamethylcalix[4]pyrrole (OMCP), and its interactions with the halide anions F^-, Cl^-, and Br^- and the cesium halides CsF, CsCl, and CsBr have been performed. Geometries, binding energies, and binding enthalpies were evaluated with the restricted hybrid Becke three-parameter exchange functional (B3LYP) method using the 6-31+G(d) basis set and relativistic effective core potentials. The optimized geometric structures were used to perform natural bond orbital (NBO) analysis. The two typical types of hydrogen bonds, N–H…X^- and C–H…X^-, were investigated. The results indicate that hydrogen bonding interactions are dominant, and that the halide anions (F^-, Cl^-, and Br^-) offer lone pair electrons to the σ*(N–H) or σ*(C–H) antibonding orbitals of OMCP. In addition, electrostatic interactions between the lone pair electrons of the halide anion and the LP* orbitals of Cs^+ as well as cation–π interactions between the metal ion and π-orbitals of the pyrrole rings have important roles to play in the Cs^+•OMCP•X^- complexes. The current study further demonstrates that this easy-to-make OMCP host compound functions as not only an anion receptor but also an ion-pair receptor.

Keywords Density functional theory (DFT) · Ion-pair receptor · Meso-octamethylcalix[4]pyrrole (OMCP) · Natural bond orbital (NBO)

Y. Xia · X. Wang (✉) · Y. Zhang · B. Luo · Y. Liu
Key Laboratory of Environmentally Friendly Chemistry and Applications of Ministry of Education, College of Chemistry, Xiangtan University,
Xiangtan, Hunan 411105, People's Republic of China
e-mail: wxueye@xtu.edu.cn

Introduction

As molecular recognition has developed from its traditional preoccupation with the complexation of cations to a more comprehensive view that includes the recognition of anions, it has become of interest to study systems that can simultaneously bind both cations and anions [1]. This has resulted in the synthesis of so-called ion-pair receptors, which permit the concurrent complexation of both cations and anions [2–4]. Because of their allosteric effects and enhanced electrostatic interactions between the cobound ions, ion-pair receptors are remarkably attractive materials for ion extraction, salt solubilization, and through-membrane transport [5–16].

Calix[4]pyrroles [17] are macrocyclic species with an array of four N–H bonds that act as binding sites for anionic and electron-rich neutral guests in organic solvents [18]. Interestingly, the anionic and electron-rich neutral guests organize calix[4]pyrrole into a cone conformation, which provides an electron-rich cup that putatively binds cations [19]. Previous experimental and computer modeling studies [20–25] have been carried out on this calix[4]pyrrole system. Most, if not all, of these studies have focused on anion recognition, although Custelcean [26] and Wintergerst [27] investigated the possible use of calix[4]pyrrole as a new ion-pair receptor for certain salts. The latter proposed three thermochemical steps for the solvent extraction of cesium salts, and particularly halide salts, as shown in Scheme 1. However, it would be useful to gain a deeper understanding of the interaction mechanism and the ion-pair binding properties of calix[4]pyrrole. More importantly, theoretical methods, which have become a powerful tool in supramolecular chemistry [28–31], are able to predict cooperativity effects in the binding of counterions. While there are reports of an MMFF94 force field model for a

calix[4]arene strapped calix[4]pyrrole [32], a B3LYP model for a calix[5]crown-based heteroditopic receptor [33] and a crown-ether-based heteroditopic receptor [34], and MD simulations on calix[4]arene-based heteroditopic receptors [35], to the best of our knowledge, no theoretical study of calix[4]pyrroles acting as ditopic (i.e., ion-pair) receptors has been published.

A great deal of work still needs to be done to fully understand the interaction mechanism of ditopic receptors with counterions. In particular, the nature of the ditopic receptor calix[4]pyrrole and the mechanism of its complexation are yet to be proposed. A quantum mechanical approach to this challenging endeavor should be able to make significant contributions. Thus, we performed a density functional theory (DFT) study of a new ion-pair receptor, meso-octamethylcalix[4]pyrrole (OMCP), and the results of this study are reported in the current paper.

Computational methodology

All computational calculations reported here were performed using the Gaussian 03 package [36]. The Becke three-parameter hybrid method [37] and the correlation functional of Lee, Yang, and Parr [38] (B3LYP) were used, along with the 6-31+G(d) basis set for C, H, N, F, Cl, and Br atoms and the Lanl2dz basis set for Cs, with the latter including a double-ζ valence basis set with the Hay and Wadt effective core potential (ECP) [39, 40]. Stationary structures were obtained by verifying that all of the harmonic frequencies were real. The default options were employed for all optimizations. No symmetry constraints were imposed during the optimizations. Natural bond orbital (NBO) analysis was carried out with NBO 3.1 implemented in Gaussian 03.

Generally, the basis set superposition error (BSSE) correction should be included in order to obtain an accurate interaction energy [41]. In this study, the interaction energy was very strong, mainly because of the electrostatic interactions. However, the basis set superposition error (BSSE), including the zero point energy (ZPE) correction, was also considered in the binding energy calculations. The most popular method of correcting for the BSSE—the counterpoise (CP) correction technique proposed by Boys and Bernardi [42]—was used.

Results and discussion

Structural analysis of OMCP and its complexes

Calix[4]pyrroles—like a related family of compounds, the calix[4]arenes—are very flexible, because rotation can occur around the interpyrrole bonds. Theoretical calculations [24] indicate that calix[4]pyrrole can adopt four major conformations: a cone, a partial cone, a 1,2-alternate, and a 1,3-alternate. The current study attempted to optimize all

Scheme 1 Previously proposed steps in cesium salt extraction

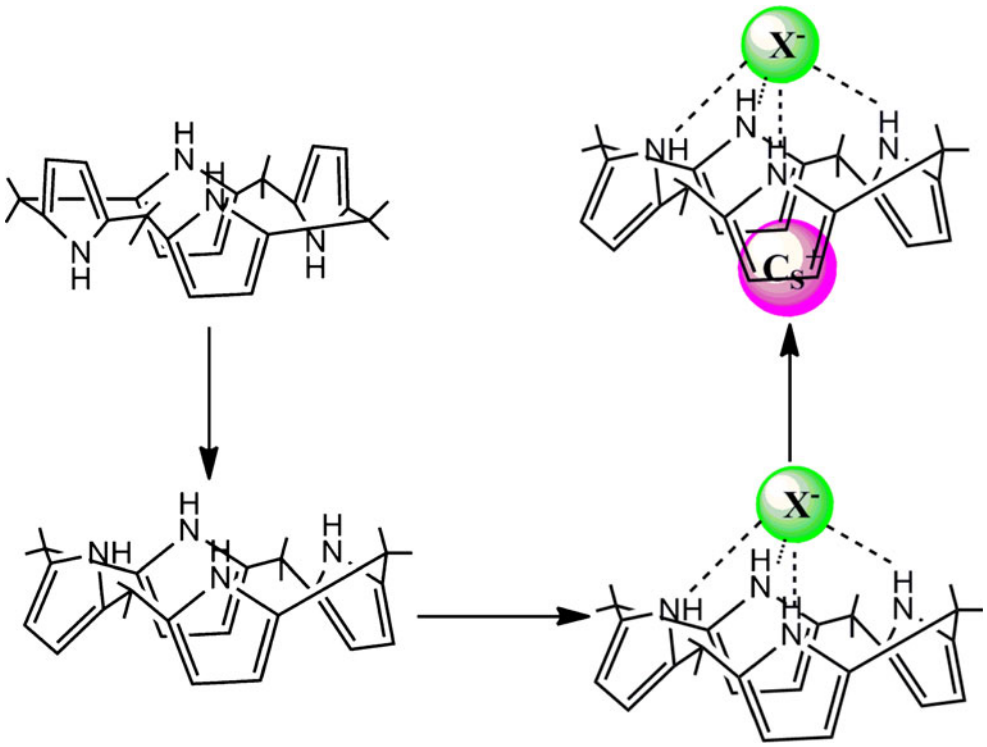

four putative conformations of meso-octamethylcalix[4]pyrrole (OMCP, shown in Fig. 1a). However, a stable structure was found for only one of these conformers (Fig. 1b), the 1,3-alternate conformer, in remarkable agreement with the X-ray structure [20]. This situation presumably arises because of steric interactions involving the meso-methyl groups. Thus, the 1,3-alternate conformer was chosen for further investigations. The obtained optimized geometries of the ligand OMCP and its complexes are shown in Figs. 1, 2, and 3, respectively. Corresponding vibrational frequency calculations indicated that all of the optimized structures appear to be true minima.

The calculated geometrical parameters of the 1,3-alternate conformation of meso-octamethylcalix[4]pyrrole (OMCP), obtained using the B3LYP method with four different basis sets [6-31G, 6-31+G, 6-31+G(d) and 6-31+G (d,p)], as well as the corresponding values for the X-ray crystal structure of OMCP are provided in Table 1. Inspecting Table 1, it is clear that the basis set used makes little difference to the calculated structure parameters. The calculated structures agree with the X-ray structure very well; in particular, the calculated total energy, as expected, decreases considerably with the size of the basis set. The calculated bond lengths generally exceed the X-ray values by no more than 0.01 Å, and the calculated bond angles and dihedral angles are within 0.05° of the experimental values, except for ∠N2-C4-C5-C6 and ∠C4-C5-C6-N3. The above results illustrate that the results of the current study are very reliable, and that 6-31+G(d) is the optimal choice of basis set to model our system. Therefore, the remaining data reported in this paper were obtained with the 6-31+G(d) basis set.

The experimental data show that the cone conformation is the most populated form when the calix[4]pyrroles form 1:1 complexes with small anions [17, 20, 26]. Upon inspecting Figs. 2 and 3, it is clear that our calculations indicate that small halide ions organize meso-octamethylcalix[4]pyrrole (OMCP) into the cone conformation, which in turn provides an electron-rich cup that putatively binds the Cs^+ ion. Selected geometrical parameters of OMCP•X^- and Cs^+•OMCP•X^- (X=F^-, Cl^-, and Br^-) obtained using the B3LYP/6-31+G(d) method, as well as the corresponding values from their X-ray crystal structures, are provided in Tables 2 and 3, respectively.

As a first step towards understanding the ion-pair binding properties of meso-octamethylcalix[4]pyrrole (OMCP), the complexes of OMCP with halide anions (F^-, Cl^-, and Br^-) were studied in detail. Inspecting Fig. 2 and Table 2, it is clear that these halide anion complexes adopt the cone conformation with the anion sitting above the cone, and form four hydrogen bonds with the four pyrrole N–Hs. Furthermore, it appears that the halide anion is located at the center of the complex, as indicated by the almost identical X^-…H distances. The lengths of the hydrogen bonds are different in different complexes; the average values are 1.74, 2.32, and 2.46 Å for OMCP•F^-, OMCP•Cl^-, and OMCP•Br^-, respectively. The calculated results indicate that the hydrogen-bond interactions in OMCP•F^- may be stronger than those in the other complexes. Because of the NH…X^- hydrogen bonds, meso-octamethylcalix[4]pyrrole (OMCP) is flattened to different degrees in the complexes, as indicated by the different typical dihedral angles (φ, χ, ψ, and ω). The calculated average value for the nitrogen–chloride ion distance is 3.338 Å, which is in remarkable agreement with the experimental data (which indicate values in the range of 3.264(7)–3.331(7)) [20]. The Cs^+•OMCP•X^- (X=F^-, Cl^-, and Br^-) complexes were then studied. In the Cs^+•OMCP•F^- complex, the cation is symmetrically enveloped in the conelike cavity of the meso-octamethylcalix[4]pyrrole unit (Fig. 3a); the observed distance between the Cs^+ ion and the centroid of each pyrrole rings is 3.56 Å (the

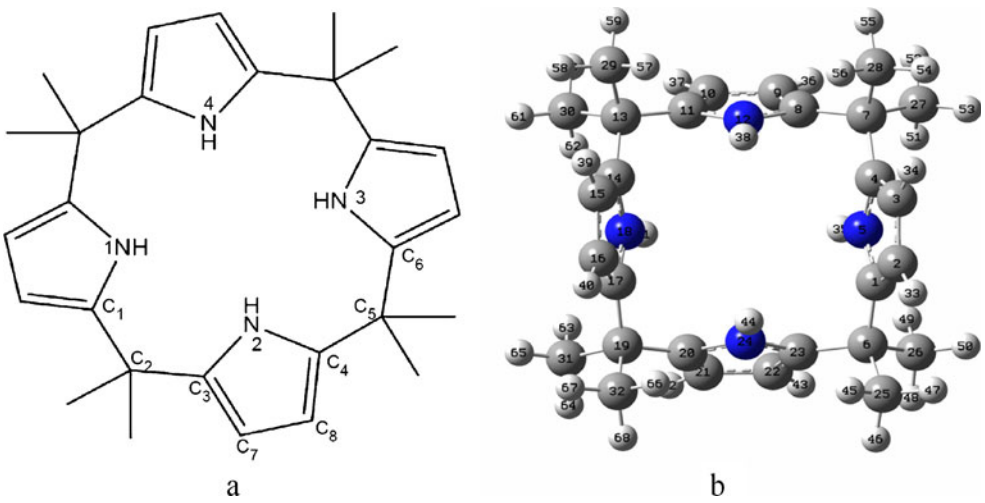

Fig. 1 Chemical structures of the investigated OMCP: **a** the sketch map (the atom numbering was used for reference purposes in structural analysis only; it is not systematic); **b** the optimized structure based on B3LYP/6-31 +G(d) (the atom numbering was used for NBO analysis only; it is not systematic)

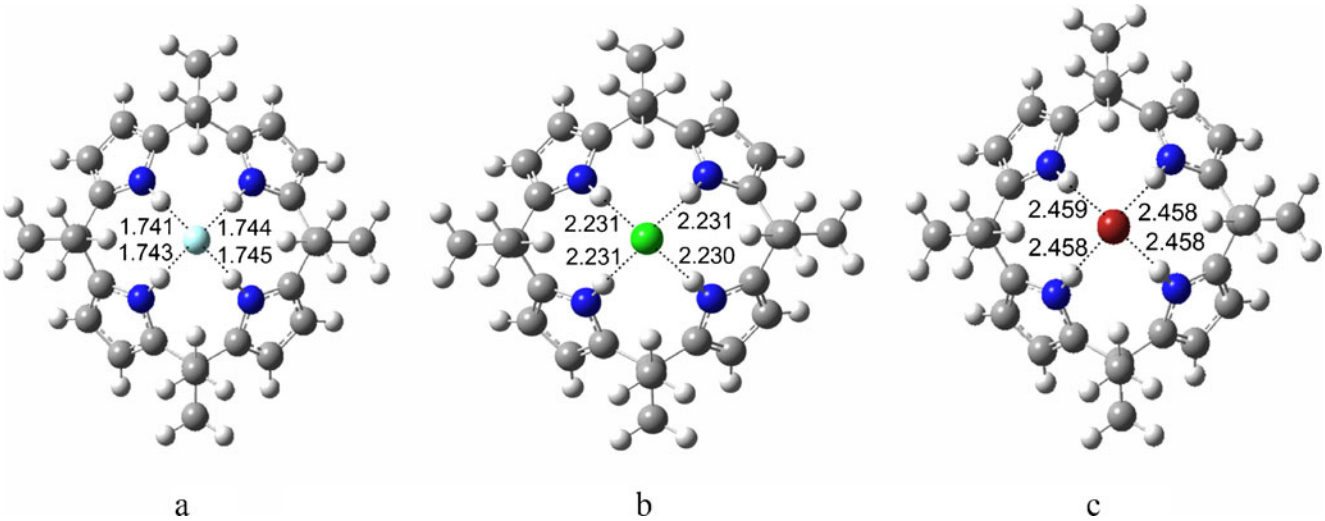

Fig. 2 The optimized structures of the complexes calculated at the B3LYP/6–31+G(d) level: **a** OMCP•F^-, **b** OMCP•Cl^-, and **c** OMCP•Br^-

corresponding value from the X-ray structure is 3.39 Å [26]). The F^- ion is symmetrically bound to the four NH groups of the meso-octamethylcalix[4]pyrrole, and the N…F^- interaction occurs at a distance of 2.74 Å (this distance is slightly shorter than that seen in the OMCP•F^- complex, as shown in Tables 2 and 3). The Cs^+ ion is tightly bound by the cone-shaped meso-octamethylcalix[4]pyrrole, with observed distances of 3.57 and 3.50 Å to the centroids of the pyrrole rings for the Cs^+•OMCP•Cl^- (Fig. 3b) and Cs^+•OMCP•Br^- (Fig. 3c) complexes, respectively. The Cl^- and Br^- ions are

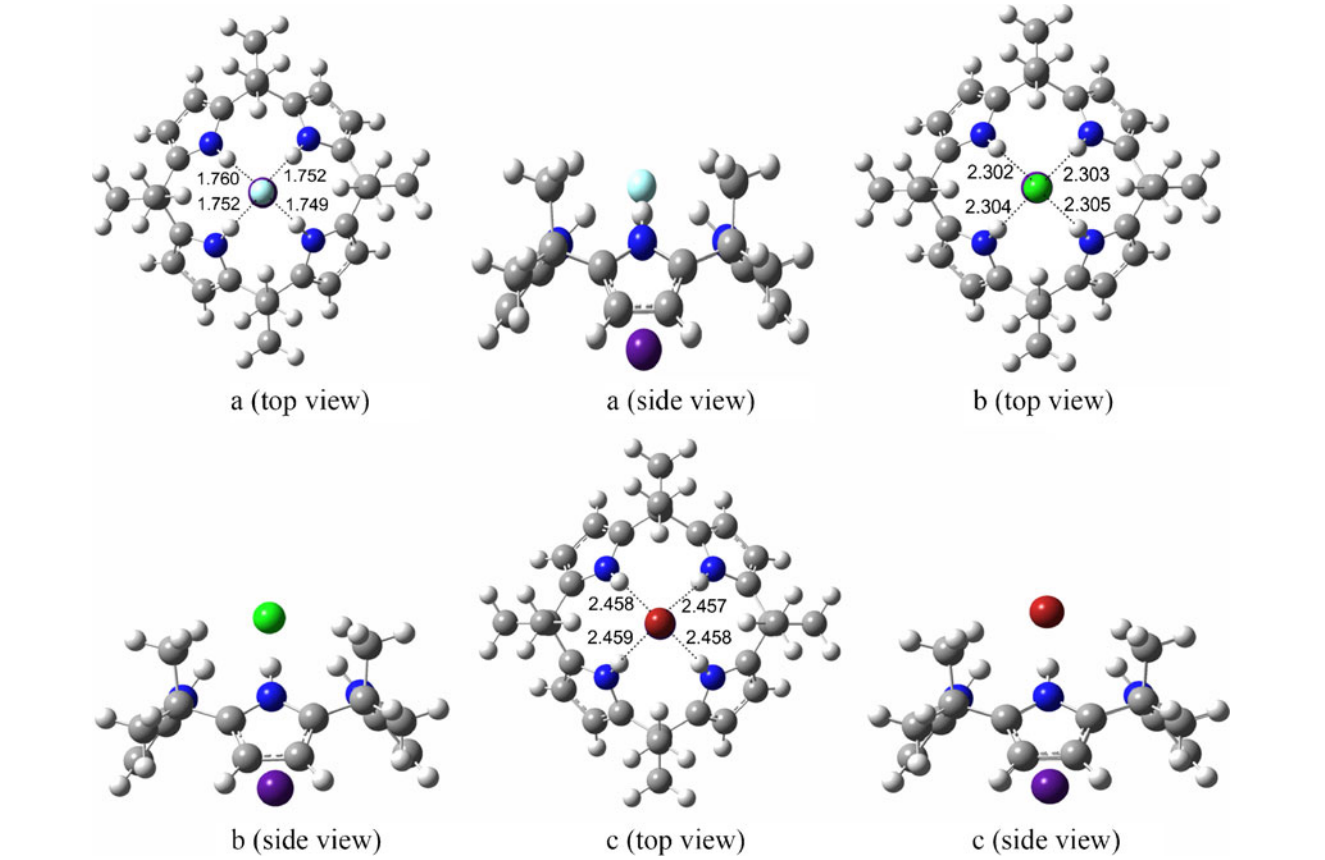

Fig. 3 The optimized structures of the complexes calculated at the B3LYP/6–31+G(d) level: **a** Cs^+•OMCP•F^-, **b** Cs^+•OMCP•Cl^-, and **c** Cs^+•OMCP•Br^-, respectively

Table 1 Selected structure parameters (distances in Å and angles in degrees) and calculated energies for OMCP optimized using the B3LYP method with four different basis sets [6-31G, 6-31+G, 6-31+G(d) and 6-31+G(d,p)], as well as the experimental values of the same parameters obtained from the X-ray crystal structure

	6-31G	6-31+G	6-31+G(d)	6-31+G(d,p)	X-ray
r(N1-C1)	1.391	1.392	1.381	1.381	1.375
r(C2-C3)	1.521	1.522	1.520	1.520	1.521
∠N1-C1-C2	121.0	121.1	121.0	121.0	121.0
∠C1-C2-C3	110.1	110.0	109.9	109.9	109.5
∠C3-N2-C4	110.7	110.8	111.0	111.0	110.7
∠N2-C4-C5	121.0	121.1	121.0	121.0	121.0
∠N1-C1-C2-C3	−51.2	−51.5	−52.7	−52.8	−50.3
∠C1-C2-C3-N2	−55.8	−56.0	−56.8	−56.7	−57.3
∠C2-C3-N2-C4	−178.2	−178.4	−178.9	−178.9	−178.6
∠C3-N2-C4-C5	177.3	177.4	177.9	177.9	176.8
∠N2-C4-C5-C6	51.2	51.5	52.7	52.8	48.3
∠C4-C5-C6-N3	55.8	56.0	56.8	56.7	59.2
energy (a.u.)	−1307.33950	−1307.38071	−1307.70924	−1307.7684	–

bound to the four NH groups of the meso-octamethylcalix[4]pyrrole by hydrogen bonds; the corresponding distances are 3.30 and 3.46 Å for the N…Cl^- and N…Br^- interactions, respectively. Obviously, the N…X^- distances for the Cs^+•OMCP•X^- complexes are all shorter than those for the OMCP•X^- complexes, and the typical dihedral angles (φ, χ, ψ, and ω) are all enlarged to different degrees. These characteristics may be attributed to the Cs^+…X^- interactions and the Cs^+–π (of the pyrrole rings) interaction. It should be noted that the Cs^+…X^- distances in CsF, CsCl, and CsBr in the solid state are 3.004, 4.118, and 4.287 Å, respectively [43]. The corresponding distances in the Cs^+•OMCP•X^- complexes are longer: 3.910, 4.782, and 5.035 Å for the F^-, Cl^-, and Br^- ions, respectively. These results indicate that the Cs^+…X^- interactions in the Cs^+•OMCP•X^- complexes are weaker than those in cesium halides, and meso-octamethylcalix[4]pyrrole is a real ion-pair receptor. All of the calculated results are in remarkable agreement with the experimental data.

Table 2 Selected intermolecular parameters (distances in Å and angles in degrees) for the complexes OMCP•X^- (F^-, Cl^-, and Br^-), optimized at the B3LYP/6–31+G(d) level

	OMCP•F^-	OMCP•Cl^-	OMCP•Br^-
r(X^-–N1)	2.767	3.338	3.475
r(X^-–N2)	2.765	3.339	3.476
r(X^-–N3)	2.763	3.339	3.476
r(X^-–N4)	2.765	3.339	3.476
φ(N1–C1–C2–C3)	−70.2	−73.9	−74.5
χ(N2–C3–C2–C1)	70.4	73.9	74.5
ψ(N2–C4–C5–C6)	−70.2	−73.9	−74.5
ω(N3–C6–C5–C4)	70.4	73.9	74.5

NBO analysis

In the NBO analysis, the delocalization of electron density among occupied Lewis-type (bond or lone pair) NBO orbitals and formally unoccupied non-Lewis-type (antibond) NBO orbitals leads to stabilizing donor–acceptor interactions, which are taken into account by examining the possible interactions between filled (donor) Lewis-type NBOs and empty (acceptor) non-Lewis NBOs and then estimating their energies by second-order perturbation theory. For each donor NBO (i) and acceptor NBO (j), the stabilization energy (E_2)

Table 3 Selected intermolecular parameters (distance in Å and angles in degrees) for the complexes Cs^+•OMCP•X^- (F^-, Cl^-, and Br^-), optimized at the B3LYP/6–31+G(d) level[a]

	Cs^+•OMCP•F^-	Cs^+•OMCP•Cl^-	Cs^+•OMCP•Br^-
r(X^-–N1)	2.743	3.300	3.463
r(X^-–N2)	2.748	3.300	3.463
r(X^-–N3)	2.752	3.301	3.464
r(X^-–N4)	2.748	3.302	3.464
φ(N1–C1–C2–C3)	−75.3	−77.6	−77.3
χ(N2–C3–C2–C1)	74.4	77.5	77.5
ψ(N2–C4–C5–C6)	−74.4	−77.6	−77.5
ω(N3–C6–C5–C4)	75.0	77.5	77.5
r(X^-–Cs^+)	3.910 (3.69)	4.782 (4.68)	5.035 (4.95)

[a] The experimentally determined distances *r*(X^-–N) in the complexes Cs^+•OMCP•F^-, Cs^+•OMCP•Cl^-, and Cs^+•OMCP•Br^- complexes were 2.79, 3.32–3.79, and 3.34–3.51 Å, respectively. The values given in parentheses are the experimental data. All experimental data were obtained from [19]

associated with $i \rightarrow j$ delocalization can be explicitly estimated using the following equation:

$$E_2 = \Delta E_{ij} = q_i \frac{F^2(i,j)}{\varepsilon_j - \varepsilon_i}, \quad (1)$$

where q_i is the i^{th} donor orbital occupancy, ε_i and ε_j are diagonal elements (orbital energies), and $F(i, j)$ are off-diagonal elements associated with the NBO Fock matrix.

The hydrogen bond interaction energies are between 0.5 and 2.0 kcal mol^{-1}, which are typical of weak hydrogen bonds [44]. Due to the strong host–guest interactions in the OMCP•X$^-$ (X=F$^-$, Cl$^-$, and Br$^-$) complexes, only hydrogen bond interaction energies of >2.0 kcal mol^{-1} were considered in the current study. The second-order perturbation stabilization energies E_2 obtained from NBO analysis of both OMCP•X$^-$ and Cs$^+$•OMCP•X$^-$ (X=F$^-$, Cl$^-$, and Br$^-$) are summarized in Tables 4 and 5. NBO analysis indicates that the interaction energies E_2 of the host–guest molecules OMCP•X$^-$ are mainly caused by the lone pair electrons of the halide anion and the σ* (two-center antibonding) orbitals of the N–H bonds or C–H bonds in OMCP. In addition, the LP* (one-center valence antibonding lone pair) orbital of the cesium cation contributes to the E_2 in Cs$^+$•OMCP•X$^-$ complexes.

Inspecting Table 4, it is clear that there are strong donor–acceptor interactions between the lone pair electrons of the anion F$^-$ and the σ* orbitals of N5–H35, N12–H38, N18–H41, and N24–H44 in the OMCP•F$^-$ complex, and the maximum E_2 reaches 20.47 kcal mol^{-1}. However, the corresponding values of E_2 are much lower in the OMCP•X$^-$ (X=Cl$^-$ and Br$^-$) complexes. It is well known that the larger the stabilization interaction energy E_2 between a donor bonding orbital and an acceptor antibonding orbital, the stronger the interaction between the two bonds. Thus, if we arrange the host–guest interactions for the complexes OMCP•X$^-$ in descending order of interaction strength, we get OMCP•F$^-$>OMCP•Cl$^-$>OMCP•Br$^-$. It should be noted that the values of E_2 between the lone pair electrons of the halide anion and the σ* orbitals of C–H bonds exceed 2.0 kcal mol^{-1} in the OMCP•X$^-$ (X=Cl$^-$ and Br$^-$) complexes. Therefore, there are strong C–H…X$^-$ hydrogen bonds in the OMCP•Cl$^-$ and OMCP•Br$^-$ complexes. These may result from the larger ionic radius (compared to F$^-$), which shortens the distance between the lone pair electrons of the halide anion and the adjacent σ* orbitals of C–H bonds. Inspecting Table 5, it is clear that the hydrogen bond interaction energies are little changed in the Cs$^+$•OMCP•X$^-$ complexes compared with the OMCP•X$^-$ complexes (except for Cs$^+$•OMCP•F$^-$). In the Cs$^+$•OMCP•X$^-$ complexes, there are interactions between the lone pair electrons of the halide anion and the LP* orbitals of Cs$^+$, as well as cation–π (of the pyrrole rings) interactions. It is interesting that the E_2 values of the cation–π interactions are very similar across the Cs$^+$•OMCP•X$^-$ complexes (about 0.64 kcal mol^{-1}). In addition, the E_2 value for the interactions of the lone pair electrons of the halide anion with the LP* orbitals of Cs$^+$, which are 0.31–0.97 kcal mol^{-1} in the Cs$^+$•OMCP•X$^-$ complexes, are much smaller than the corresponding values for isolated cesium halides. These results can be explained by the concurrent complexation of both the cesium cation and the halide anion; i.e., meso-

Table 4 Selected stabilization interaction energies E_2 (kcal mol^{-1}) for OMCP•X$^-$ (F$^-$, Cl$^-$, and Br$^-$) complexes

Complexes	Donor NBO(i) → acceptor NBO(j)	E_2	Donor NBO(i) → acceptor NBO(j)	E_2	Donor NBO(i) → acceptor NBO(j)	E_2
OMCP•F$^-$	LP2 F → σ*N5–H35	8.44	LP2 F → σ*N12–H38	3.62	LP2 F → σ*N18–H41	9.42
	LP2 F → σ*N24–H44	16.51	LP3 F → σ*N5–H35	10.21	LP2 F → σ*N18–H41	14.13
	LP4 F → σ*N5–H35	5.31	LP4 F → σ*N12–H38	20.47		
OMCP•Cl$^-$	LP2 Cl → σ*N5–H35	3.56	LP2 Cl → σ*N12–H38	2.77	LP2 Cl → σ*N18–H41	3.55
	LP2 Cl → σ*N24–H44	2.77	LP2 Cl → σ*C26–H49	2.01	LP2 Cl → σ*C30–H62	2.02
	LP3 Cl → σ*N5–H35	2.76	LP3 Cl → σ*N12–H38	3.56	LP3 Cl → σ*N18–H41	2.78
	LP3 Cl → σ*N24–H44	3.55	LP3 Cl → σ*C27–H51	2.00	LP3 Cl → σ*C31–H63	2.01
	LP4 Cl → σ*N5–H35	7.18	LP4 Cl → σ*N12–H38	7.20	LP4 Cl → σ*N18–H41	7.18
	LP4 Cl → σ*N24–H44	7.16				
OMCP•Br$^-$	LP2 Br → σ*N5–H35	2.82	LP2 Br → σ*N12–H38	2.78	LP2 Br → σ*N18–H41	2.81
	LP2 Br → σ*N24–H44	2.78	LP2 Br → σ*C26–H49	2.74	LP2 Br → σ*C30–H62	2.75
	LP3 Br → σ*N5–H35	2.78	LP3 Br → σ*N12–H38	2.82	LP3 Br → σ*N18–H41	2.79
	LP3 Br → σ*N24–H44	2.82	LP3 Br → σ*C26–H49	2.74	LP3 Br → σ*C30–H62	2.74
	LP4 Br → σ*N5–H35	7.21	LP4 Br → σ*N12–H38	7.23	LP4 Br → σ*N18–H41	7.21
	LP4 Br → σ*N24–H44	7.19				

LP one-center valence lone pair (LP1-sp0.05 is the lone pair NBO in the plane; LP2-sp35.01, LP3-sp99.99, and LP4-sp60.59 are the corresponding NBOs perpendicular to the plane); *σ** two-center antibonding

Table 5 Selected stabilization interaction energies E_2 (kcal mol^{-1}) for Cs^+•OMCP•X^- (F^-, Cl^-, and Br^-) complexes

Complexes	Donor NBO(*i*) → acceptor NBO (*j*)	E_2	Donor NBO(*i*) → acceptor NBO (*j*)	E_2	Donor NBO(*i*) → acceptor NBO (*j*)	E_2
Cs^+•OMCP•F^-	LP2 F → σ*N5–H35	8.74	LP2 F → σ*N12–H38	8.88	LP2 F → σ*N18–H41	8.86
	LP2 F → σ*N24–H44	8.40	LP3 F → σ*N12–H38	12.38	LP2 F → σ*N24–H44	14.20
	LP4 F → σ*N5–H35	13.52	LP4 F → σ*N12–H38	13.15	LP1 F → LP*Cs	0.31
	LP2 F → LP*Cs	0.46	BD C1–C6 → LP*Cs	0.59	BD C4–C7 → LP*Cs	0.57
	BD C6–C23 → LP*Cs	0.59	BD C7–C8 → LP*Cs	0.56	BD C11–C13 → LP*Cs	0.59
	BD C13–C14 → LP*Cs	0.59	BD C17–C19 → LP*Cs	0.59	BD C19–C20 → LP*Cs	0.59
Cs^+•OMCP•Cl^-	LP2 Cl → σ*N5–H35	3.56	LP2 Cl → σ*N12–H38	2.77	LP2 Cl → σ*N18–H41	3.55
	LP2 Cl → σ*N24–H44	2.77	LP2 Cl → σ*C26–H49	2.01	LP2 Cl → σ*C30–H62	2.02
	LP3 Cl → σ*N5–H35	2.76	LP3 Cl → σ*N12–H38	3.56	LP3 Cl → σ*N18–H41	2.78
	LP3 Cl → σ*N24–H44	3.55	LP3 Cl → σ*C27–H51	2.00	LP3 Cl → σ*C31–H63	2.01
	LP4 Cl → σ*N5–H35	7.18	LP4 Cl → σ*N12–H38	7.20	LP4 Cl → σ*N18–H41	7.18
	LP4 Cl → σ*N24–H44	7.16	LP4 Cl → LP*Cs	0.75	LP1 Cl → LP*Cs	0.76
	BD C6–C23 → LP*Cs	0.64	BD C7–C8 → LP*Cs	0.62	BD C11–C13 → LP*Cs	0.64
	BD C13–C14 → LP*Cs	0.64	BD C17–C19 → LP*Cs	0.65	BD C19–C20 → LP*Cs	0.64
	BD C4–C7 → LP*Cs	0.61	BD C1–C6 → LP*Cs	0.63		
Cs^+•OMCP•Br^-	LP2 Br → σ*N5–H35	3.63	LP2 Br → σ*N12–H38	2.76	LP2 Br → σ*N18–H41	3.68
	LP2 Br → σ*N24–H44	2.72	LP2 Br → σ*C26–H49	2.52	LP2 Br → σ*C30–H62	2.51
	LP3 Br → σ*N5–H35	2.67	LP3 Br → σ*N12–H38	3.57	LP3 Br → σ*N18–H41	2.80
	LP3 Br → σ*N24–H44	3.74	LP3 Br → σ*C27–H51	2.52	LP3 Br → σ*C30–H63	2.55
	LP4 Br → σ*N5–H35	6.99	LP4 Br → σ*N12–H38	6.95	LP4 Br → σ*N18–H41	6.77
	LP4 Br → σ*N24–H44	6.82	LP1 Br → LP*Cs	0.97	LP4 Br → LP*Cs	0.67
	BD C1–C6 → LP*Cs	0.64	BD C4–C7 → LP*Cs	0.62	BD C7–C8 → LP*Cs	0.62
	BD C11–C13 → LP*Cs	0.64	BD C13–C14 → LP*Cs	0.64	BD C17–C19 → LP*Cs	0.64

octamethylcalix[4]pyrrole (OMCP) acting as a ion-pair receptor.

Binding energies and stabilities

Further insight into the binding behavior of OMCP was gained by conveniently analyzing the binding energies, binding enthalpies, and Gibbs free energies of the OMCP•X^- and Cs^+•OMCP•X^- (X=F^-, Cl^-, and Br^-) complexes. The corresponding values were determined using the following equations:

$$\mathrm{OMCP} + \mathrm{X}^- \rightarrow \mathrm{OMCP} \bullet \mathrm{X}^- \tag{2}$$

$$\mathrm{Cs}^+ + \mathrm{OMCP} + \mathrm{X}^- \rightarrow \mathrm{Cs}^+ \bullet \mathrm{OMCP} \bullet \mathrm{X}^-. \tag{3}$$

For this system, the binding energy ΔE can be expressed as follows:

$$\Delta E = E(\mathrm{OMCP} \bullet \mathrm{X}^-) - E(\mathrm{OMCP}) - E(\mathrm{X}^-) \tag{4}$$

$$\Delta E = E(\mathrm{Cs}^+ \bullet \mathrm{OMCP} \bullet \mathrm{X}^-) - E(\mathrm{X}^-) - E(\mathrm{OMCP}) - E(\mathrm{Cs}^+). \tag{5}$$

Table 6 The binding energies ΔE (kcal mol^{-1}), binding enthalpies ΔH (kcal mol^{-1}), and Gibbs free energies ΔG (kcal mol^{-1}) in the gas phase for the complexes at 298 K[a]

	OMCP•X^-			Cs^+•OMCP•X^-		
	F^-	Cl^-	Br^-	F^-	Cl^-	Br^-
BSSE	2.54	0.68	16.20	3.69	1.75	4.77
$-\Delta E_{BSSE}$	62.73	39.15	15.32	145.15	108.64	77.90
$-\Delta E$	65.27	39.83	31.52	148.84	110.39	82.67
$-\Delta H$	66.05	40.42	32.11	149.67	111.58	83.86
$-\Delta G$	55.17	29.69	21.69	130.27	92.49	70.23

[a] The binding energy icludes corrections for the ZPE and BSSE

The thermodynamic data calculated using the above equations at the B3LYP/6-31+G(d) level are reported in Table 6.

In the OMCP•X^- complexes, the calculated thermal energy increases with the size of the halide anion (F^-, Cl^-, and Br^-), meaning that ΔE (OMCP•F^-)<ΔE (OMCP•Cl^-) <ΔE (OMCP•Br^-). This can be explained by the strong host–guest interactions. It is well known that the higher the

electronegativity and electron density, the stronger the hydrogen-bonding interactions. Due to the different properties of the three halide anions, the formation of intermolecular hydrogen bonds becomes more difficult as we move from F^- to Cl^- to Br^-. That is to say, it is much easier to form an intermolecular hydrogen bond with an F^- ion than with Cl^- or Br^- under the same conditions. This is also consistent with the structure analysis, which established that the hydrogen-bond distances increase from F^- to Br^- (shown in Table 2). The experimental data also indicated that the sequence of stabilities was OMCP•F^-> OMCP•Cl^->OMCP•Br^- [20].

The calculated thermal energies for the Cs^+•OMCP•X^- complexes change monotonously with the size of the halide anion (F^-, Cl^-, and Br^-), meaning that ΔE (Cs^+•OMCP•F^-) <ΔE (Cs^+•OMCP•Cl^-)<ΔE (Cs^+•OMCP•Br^-). However, the experimental data indicated that the Cs^+OMCP•Br^- complex is more stable than the Cs^+OMCP•Cl^- complex (no experimental data were available for Cs^+OMCP•F^-) [27]. It is clear that the order of the calculated binding energies for the Cs^+•OMCP•X^- complexes is not consistent with the experimental results. This difference between the theoretical calculations and experimental data results from the fact that our calculations were performed for isolated molecules in the gas phase, but the experiments were performed in solution. The solvent effect is known to influence complexation and extraction selectivities [45, 46]. Selectivity is perceptibly the result of a delicate balance of the forces that the ions experience as the OMCP and solvent molecules compete for the ions in solution. In solution, the anion's binding affinity can be attenuated by anion hydration, and the hydration numbers differ among the halide anions (F^-, Cl^-, and Br^-) [47]. Since this water of hydration is presumably partially lost upon binding, the energetic cost of this process is expected to vary with the anion too. However, since Cs^+ is only minimally hydrated in water-saturated organic solvent [47], there is little or no dehydration penalty to pay when it is bound within the calix-like bowl. In addition, the solvent effect plays an important role in the stabilization of a particular isomer. Generally speaking, the most favorable isomer in the vacuum may not be the most preferred isomer in the solution. The vacuum and nonpolar solvents stabilize structures of low polarity, but increasing the polarity of the solution leads to the stabilization of polar structures.

Conclusions and perspectives

DFT calculations were performed using the B3LYP method at the 6-31+G(d) level in order to determine the electronic and geometrical structures of the ligand OMCP and the OMCP•X^- and Cs^+•OMCP•X^- (X=F^-, Cl^-, and Br^-) complexes. Interestingly, it was found that halide anions organize OMCP into the cone conformation, which then in turn provides an electron-rich cup that putatively binds the Cs^+ ion. These calculated results are in remarkable agreement with the data obtained from the X-ray crystal structures.

NBO analysis illustrated that the large stabilization interaction energies E_2 are caused by interactions of the lone pair electrons of the halide anion with the σ* (two-center antibonding) orbitals of the N–H bonds or C–H bonds in the OMCP•X^- complexes. In addition, there are interactions between the lone pair electrons of the halide anion and the LP* orbitals of Cs^+, and cation–π (of the pyrrole rings) interactions in the Cs^+•OMCP•X^- complexes. Thermal energy analysis indicated that the very high stabilities of the OMCP•X^- and Cs^+•OMCP•X^- complexes reflect the strong interactions between the host–guest molecules. Poor agreement of the calculated thermal energies of the Cs^+•OMCP•X^- complexes with the experimental results mentioned earlier can be attributed to the solvent effect.

The present study has further demonstrated that the easy-to-make meso-octamethylcalix[4]pyrrole host compound functions not only as an anion receptor but also as an ion-pair receptor. In particular, it may guide the design of more sophisticated and elaborate ion-pair receptors, and inspire a series of new applications for calix[4]pyrroles, such as building blocks for crystal engineering, molecular membranes, and anion–cation extractions. Studies of these and other possibilities are currently underway in the scientific community.

References

1. Kim SK, Sessler JL (2010) Chem Soc Rev 39:3784–3809
2. Cametti M, Nissinen M, Dalla Cort A, Mandolini L, Rissanen K (2007) J Am Chem Soc 129:3641–3648
3. Lankshear MD, Dudley IM, Chan KM, Beer PD (2007) New J Chem 31:684–690
4. Dehaen W, Gale PA, García-Garrido SE, Kostermans M, Light ME (2007) New J Chem 31:691–696
5. Tong CC, Quesada R, Sessler JL, Gale PA (2008) Chem Commun 6321–6323
6. Davis AP, Sheppard DN, Smith BD (2007) Chem Soc Rev 36:348–357
7. Pfeifer JR, Reiss P, Koert U (2006) Angew Chem Int Edn 45:501–504
8. Sisson AL, Shah MR, Bhosale S, Matile S (2006) Chem Soc Rev 35:1269–1286
9. Mahoney JM, Stucker KA, Jiang H, Carmichael I, Brinkmann NR, Beatty AM, Noll BC, Smith BD (2005) J Am Chem Soc 127:2922–2928
10. Gokel GW, Leevy WM, Weber ME (2004) Chem Rev 104:2723–2750
11. Chrisstoffels LAJ, De Jong F, Reinhoudt DN, Sivelli S, Gazzola L, Casnati A, Ungaro R (1999) J Am Chem Soc 121:10142–10151

12. Rudkevich DM, Mercer-Chalmers JD, Verboom W, Ungaro R, Reinhoudt DN (1999) J Am Chem Soc 117:6124–6125
13. Deetz MJ, Shang M, Smith BD (2000) J Am Chem Soc 122:6201–6207
14. Mahoney JM, Beatty AM, Smith BD (2004) Inorg Chem 43:7617–7621
15. Mahoney JM, Davis JP, Smith BD (2003) J Org Chem 68:9819–9820
16. Mahoney JM, Beatty AM, Smith BD (2001) J Am Chem Soc 123:5847–5858
17. Gale PA, Sessler JL, Král V (1998) Chem Commun 1–8
18. Allen WE, Gale PA, Brown CT, Lynch VM, Sessler JL (1996) J Am Chem Soc 118:12471–12472
19. Anzenbacher P Jr, Jursíková K, Lynch VM, Gale PA, Sessler JL (1999) J Am Chem Soc 121:11020–11021
20. Gale PA, Sessler JL, Král V, Lynch V (1996) J Am Chem Soc 118:5140–5141
21. Gale PA, Garcıa-Garrido SE, Garric J (2008) Chem Soc Rev 37:151–190
22. Sessler JL, Gross DE, Cho WS, Lynch VM, Schmidtchen FP, Bates GW, Light ME, Gale PA (2006) J Am Chem Soc 128:12281–12288
23. Kim SK, Gross DE, Cho DG, Lynch VM, Sessler JL (2011) J Org Chem 76:1005–1012
24. Blas JR, Márquez M, Sessler JL, Luque FJ, Orozco M (2002) J Am Chem Soc 124:12796–12805
25. Wu YD, Wang DF, Sessler JL (2001) J Org Chem 66:3739–3746
26. Custelcean R, Delmau LH, Moyer BA, Sessler JL, Cho WS, Gross D, Bates GW, Brooks SJ, Light ME, Gale PA (2005) Angew Chem Int Edn 44:2537–2542
27. Wintergerst MP, Levitskaia TG, Moyer BA, Sessler JL, Delmau LH (2008) J Am Chem Soc 130:4129–4139
28. Sheehan R, Cragg PJ (2008) Supramol Chem 20:443–451
29. Yan S, Lee SJ, Kang S, Lee JY (2007) Supramol Chem 19:229–241
30. Mohammed-Ziegler I, Billes FJ (2007) Incl Phenom Macrocycl Chem 58:19–42
31. Schatz J (2004) Collect Czech Chem Commun 69:1169–1194
32. Kim SK, Sessler JL, Gross DE, Lee CH, Kim JS, Lynch VM, Delmau LH, Hay BP (2010) J Am Chem Soc 132:5827–5836
33. Gargiulli C, Gattuso G, Notti A, Pappalardo S, Parisi MF (2010) Supramol Chem 22:358–364
34. Vivas-Reyes R, De Proft F, Biesemans M, Willem R, Geerlings P (2003) Eur J Inorg Chem 1315–1324
35. Lankshear MD, Dudley IM, Chan KM, Cowley AR, Santos SM, Felix V, Beer PD (2008) Chem Eur J 14:2248–2263
36. Frisch MJ, Trucks GW, Schlegel HB, Scuseria GE, Robb MA, Cheeseman JR, Montgomery JA Jr, Vreven T, Kudin KN, Burant JC, Millam JM, Iyengar SS, Tomasi J, Barone V, Mennucci B, Cossi M, Scalmani G, Rega N, Petersson GA, Nakatsuji H, Hada M, Ehara M, Toyota K, Fukuda R, Hasegawa J, Ishida M, Nakajima T, Honda Y, Kitao O, Nakai H, Klene M, Li X, Knox JE, Hratchian HP, Cross JB, Adamo C, Jaramillo J, Gomperts R, Stratmann RE, Yazyev O, Austin AJ, Cammi R, Pomelli C, Ochterski JW, Ayala PY, Morokuma K, Voth GA, Salvador P, Dannenberg JJ, Zakrzewski VG, Dapprich S, Daniels AD, Strain MC, Farkas O, Malick DK, Rabuck AD, Raghavachari K, Foresman JB, Ortiz JV, Cui Q, Baboul AG, Clifford S, Cioslowski J, Stefanov BB, Liu G, Liashenko A, Piskorz P, Komaromi I, Martin RL, Fox DJ, Keith T, Al-Laham MA, Peng CY, Nanayakkara A, Challacombe M, Gill PMW, Johnson B, Chen W, Wong MW, Gonzalez C, Pople JA (2003) Gaussian 2003W, revision B. 05. Gaussian Inc., Pittsburgh
37. Becke AD (1993) J Chem Phys 98:5648–5652
38. Lee C, Yang W, Parr RP (1988) Phys Rev B 37:785–789
39. Wadt WR, Hay PJ (1985) J Chem Phys 82:284–298
40. Hay PJ, Wadt WR (1985) J Chem Phys 82:299–310
41. Jansen HB, Ros P (1969) Chem Phys Lett 3:140–143
42. Boys SF, Bernardi F (1970) Mol Phys 19:553–566
43. Davey WP (1923) Phys Rev 21:143–161
44. Uccello-Barretta G, Balzano F, Sicoli G, Paolino D, Guccione S (2004) Bioorg Med Chem 12:447–458
45. Glendening ED, Feller D, Thompson MA (1994) J Am Chem Soc 116:10657–10669
46. Zheng XY, Wang XY, Yi SF, Wang NQ, Peng YM (2010) J Comput Chem 31:1458–1468
47. Osakai T, Ogata A, Ebina K (1997) J Phys Chem B 101:8341–8348